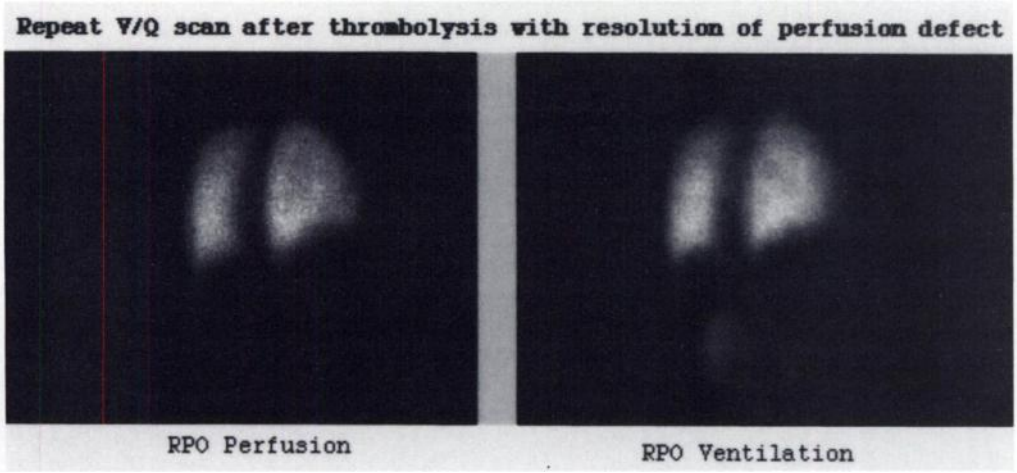

FIGURE 3. A repeat V/Q study after thrombolysis showing resolution of the right middle lobe perfusion abnormality.

could also be mimicked by normally perfused tissue in segments adjacent to the lesion or in the contralateral lung. This may be incorrectly interpreted as a less-suspicious, nonpleural-based lesion, and the patient may not get proper treatment. Under these circumstances, SPECT imaging is less likely to misrepresent pleural contact in perfusion lesions and should be considered when performing V/Q studies.

REFERENCES

1. Sostman HD, Gottschalk A. The stripe sign: a new sign for diagnosis of nonembolic defects on pulmonary scintigraphy. *Radiology* 1982;142:737-741.
2. Sostman HD, Gottschalk A. Prospective validation of the stripe sign in ventilation-perfusion scintigraphy. *Radiology* 1992;184:455-459.
3. The PIOPED investigators. Value of the ventilation/perfusion scan in acute pulmonary embolism: results of the prospective investigation of pulmonary embolism diagnosis (PIOPED). *JAMA* 1990;263:2753-2759.

Early Detection of Bleomycin-Induced Lung Injury in Rat Using Indium-111-Labeled Antibody Directed Against Intercellular Adhesion Molecule-1

Ronald E. Weiner, Daniel E. Sasso, Maria A. Gionfriddo, Sergei I. Syrbu, Henry M. Smilowitz, John Vento and Roger S. Thrall

Departments of Diagnostic Imaging and Therapeutics, Medicine, Surgery and Pharmacology, University of Connecticut Health Center, Farmington, Connecticut; and Department of Radiology, VA Medical Center, Newington, Connecticut

We have investigated whether an ^{111}In-labeled mouse monoclonal antibody to rat intercellular adhesion molecule-1 (^{111}In*aICAM-1) could detect lung injury early in rats treated with bleomycin. **Methods:** Rats received an intravenous injection of either ^{111}In*aICAM-1 or ^{111}In-labeled normal mouse IgG (^{111}In*nmIgG) and were imaged and killed 24 hr later. Lung injury was induced by an intratracheal injection of bleomycin 4 or 24 hr before the rats were killed. After death, tissue was removed and activity was measured, lungs were cryostat-sectioned to detect the presence of ICAM-1 by immunofluorescence, and the up-regulation of LFA-1α was examined on blood polymorphonuclear leukocytes (PMNs) using fluorescence-activated cell-sorter (FACS) analysis. **Results:** In rats injected with ^{111}In*aICAM-1, the percent injected dose/organ in lungs both at 4 and 24 hr postbleomycin increased significantly compared to the values in either uninjured rats or rats that received ^{111}In*nmIgG. At 4 and 24 hr postinjury, the target-to-blood (T/B) ratio was 8/1 and 6/1, respectively. For ^{111}In*nmIgG, the T/B ratio at 4 hr was 0.5/1 and 0.4/1at 24 hr. In ^{111}In*aICAM-1 rats injured at 4 or 24 hr, images could easily be distinguished from uninjured rats. All images of ^{111}In*nmIgG rats showed only cardiac blood-pool and liver activity with little lung activity. Lung ICAM-1 immunofluorescence intensity increased in the bleomycin-treated samples compared to uninjured lungs. Expression of LFA-1α on PMNs increased 19% and 210% at 4 hr and 24 hr postinjury, respectively, compared to control values. **Conclusion:** Biodistribution and imaging data demonstrate that ^{111}In*aICAM-1 can detect early acute bleomycin-induced lung injury. Immunofluorescence and FACS data suggest that ^{111}In*ICAM-1 uptake is a specific process. This antibody has potential as an early radionuclide detector of acute inflammations.

Key Words: antiadhesion molecule antibody; acute respiratory distress syndrome; inflammation; ICAM-1

J Nucl Med 1998; 39:723-728

Indium-111 or ^{99m}Tc-labeled autologous white blood cells (WBCs) and ^{67}Ga-citrate are commonly used radiopharmaceuticals that are effective indicators of inflammatory processes in a variety of clinical settings (*1,2*). However, these agents are not without their limitations such as the time-consuming preparation and exposure to blood-borne pathogens with labeled WBCs, and low specificity and high bowel activity with ^{67}Ga. To supplant or be an adjunct to these radiopharmaceuticals, a

Received Jan. 9, 1997; revision accepted Jul. 16, 1997.

For correspondence or reprints contact: Ronald Weiner, PhD, University of Connecticut Health Center, Nuclear Medicine MC-2804, 263 Farmington Ave., Farmington, CT 06030.

wide variety of agents are under current investigation including various WBC-binding peptides (*3–6*) and WBC-binding antibodies (*7*). However, each of these is dependent on WBCs, either already at the inflammatory site or as transporter to the site. An alternative strategy that is not dependent on WBCs is to target adhesion molecules that are involved in the inflammatory process.

An important, early component in the accretion of polymorphonuclear leukocytes (PMNs) in inflammatory processes is the expression and up-regulation of adhesion molecules both on PMNs and endothelial cells (*8–10*). Expression of these molecules has been shown to be increased before PMN influx and to be associated with increased PMN-endothelial cell adhesion (*11–14*). Intercellular adhesion molecule-1 (ICAM-1) and its counterreceptor, leukocyte function associated antigen-1 (LFA-1α), are expressed constitutively on endothelial cells and PMNs, respectively. Both are up-regulated during an inflammatory process and expression of ICAM-1 is usually long-lasting with a maximum at 8–10 hr. ICAM-1 density then remains elevated for 2–7 days (*15,16*). Thus, radiolabeled antibodies directed against adhesion molecules have the potential to provide new specific diagnostic tools that theoretically should be earlier predictors of inflammation than any of the techniques currently in use, e.g., ^{67}Ga-citrate or labeled WBCs, and those agents under investigation that target WBCs.

Previously, we demonstrated that ^{111}In-labeled antirat ICAM-1 (^{111}In*aICAM-1) could detect ICAM-1 in various organs of normal rats and on cultured human umbilical endothelial cells (*17*). More importantly, this whole antibody, unlike others, is rapidly taken up by the major organs, yielding very low blood and tissue background (*17–19*). In this study, we investigated if ^{111}In*aICAM-1 could be used as an early predictor of bleomycin-induced lung injury in the rat. We report here biodistribution and imaging data of ^{111}In*aICAM-1 in animals at 4 and 24 hr following bleomycin-induced injury.

MATERIALS AND METHODS

Bleomycin Model of Lung Injury

Pathogen-free, Fischer 344 male rats (Charles River Laboratories, Worthington, MA), 200–225 g, received, under anesthesia, a single intratracheal injection of 1.5 units (~1.5 mg) bleomycin sulfate in 0.3 ml of sterile saline (*20*). Control animals received sterile saline in a similar manner.

Preparation of Indium-111-Labeled Immunoglobulins

The coupling of cyclic anhydride DTPA to each antibody, addition of ^{111}In to the antibody-DTPA complex and retention of antigen-binding ability after labeling were performed as described previously (*17*).

Biodistribution of Indium-111-Labeled Immunoglobulins

Anesthetized rats received an intravenous injection of 0.122–0.229 MBq (3.3–6.2 μCi) containing 10 μg of either ^{111}In*aICAM-1 or ^{111}In*nmIgG and were killed 24 hr after injection. Animals were injured with bleomycin at 4 or 24 hr before killing (Fig. 1). Uninjured animals served as controls. At kill, the percent injected dose/gram of tissue (%ID/g) and percent injected dose/organ (%ID/O) were determined as described by Sasso et al. (*17*).

Imaging of Indium-111-Labeled Immunoglobulins and Gallium-67

Rats received an intravenous injection of 0.76–1.48 MBq (20.5–40 μCi) containing 10–20 μg of either ^{111}In*aICAM-1 or ^{111}In*nmIgG. As an additional control, another group of rats received 20–40 μCi of ^{67}Ga-citrate suspended in 0.3 ml of saline.

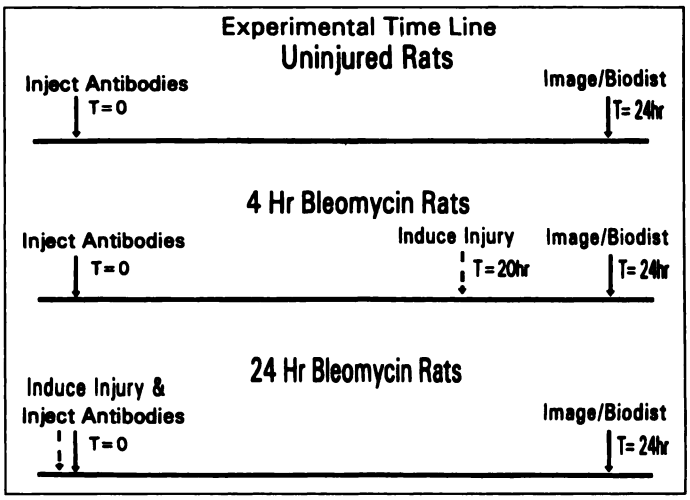

FIGURE 1. Experimental time line for the injection of ^{111}In*aICAM-1 or ^{111}In*nmIgG (solid arrow), injury with bleomycin (dotted arrow) and imaging or biodistribution (solid arrow) of the rats.

At 4 and 24 hr before imaging, the rats were injured with bleomycin and imaged in a supine position with a large field of view GE single-head gamma camera (GE Medical Systems, Milwaukee, WI) with a Digital PDP 11/40 computer and Gamma-11 software (Fig. 1). Static images were acquired using both photopeaks of ^{111}In with 15% and 20% windows on the 173-keV and 247-keV photopeaks or ^{67}Ga with 15% and 20% windows on the 93-keV and 187-keV photopeaks, respectively. A 128 × 128 word matrix was also used. Anterior views of the upper torso using a pinhole collimator were obtained and 100,000 counts were collected (~7–20 min/image). For further data analysis, the files were transferred to a Picker PCS-512 connected to a 64-bit Picker Odyssey VP computer (Picker International, Cleveland, OH). To obtain a quantitative estimate of organ and tissue localization, region of interest (ROI) analysis was used in a manner similar to Ussov et al. (*21*). ROIs were drawn around lung, liver, heart and tissue background. Care was taken to redraw the ROIs in the same position and with the same dimensions each time. High cardiac blood-pool activity in images with ^{111}In*nmIgG rats caused uncertainty in the demarcation between lung and heart. In this case, a smaller ROI was drawn to insure no overlap between tissues. For each ROI, the total counts and average counts/pixel were calculated. The counts/pixel values were divided by both the acquisition time and injected dose to normalize these values for each rat and then the normalized background activity was subtracted. For each image, ROI measurements were repeated at least three times. The percent coefficient of variation (%CV) for the individual lung measurements ranged from 6% to 31% for the ^{111}In*nmIgG rats and reflected the difficulty in the measurement. In the ^{111}In*aICAM-1 rats, the %CV for these measurements was much lower, 2%–14%. For liver and heart, the %CV was <7% with both antibodies.

Immunofluorescence of Lung Tissue

Lungs were excised and the tissues were then processed for routine fresh-frozen cryostat sectioning and the presence of ICAM-1 detected by immunofluorescence as described previously (*17*).

Flow Cytometry Detection of LFA-1α on PMNs

Whole blood was removed from the animals immediately before kill (4 or 24 hr postinjury), the cells were washed free of plasma and incubated with antirat LFA-1α (R & D Systems, Minneapolis, MN). The cells were washed, incubated with fluorescein-conjugated goat antimouse IgG (Cappel Research Products, Durham,

TABLE 1
Effect of Bleomycin-Induced Lung Injury on Organ Biodistribution of ^{111}In*aICAM-1 and ^{111}In*nmIgG in Rats

A. ^{111}In*aICAM-1	Time postbleomycin*							
	Uninjured†		4 hr‡			24 hr‡		
Tissue	%ID/O	s.d.	%ID/O	s.d.	p value¶	%ID/O	s.d.	p value¶
Lung	2.0 [2.4]§	0.2%	3.3 [4.0]	0.3%	<0.01	6.6 [7.2]	0.2%	<0.001
Blood	8.5 [0.7]	0.9%	6.8 [0.5]	0.2%	<0.05	16.6 [1.2]	2.1%	<0.001
Kidney	6.7	0.2%	3.3	0.2%	<0.001	6.5	0.5%	ns
Spleen	2.2 [3.6]	0.2%	3.1 [6.6]	0.1%	<0.01	4.0 [8.1]	0.6%	<0.001
Heart	0.18	0.2%	0.18	0.02%	ns	0.37	0.03%	<0.001
Liver	40.8	1.3%	39.1	2.6%	ns	73.1	9.3%	<0.001
Total	60.5	1.4%	55.7	2.8%	ns	107.2	11.6%	<0.001
B. ^{111}In*nmIgG								
Lung	0.9 [1.0]	0.45	0.9 [1.0]	0.3%	ns	1.5 [1.6]	0.2%	ns
Blood	32.6 [2.3]	1.4%	26.2 [1.9]	1.3%	<0.05	54.2 [3.9]	6.9%	<0.001
Kidney	2.2	0.1%	2.9	0.3%	<0.005	3.5	0.2%	0.001
Spleen	0.9 [1.6]	0.1%	0.9 [1.7]	0.1%	ns	0.9 [2.0]	0.1%	ns
Heart	0.37	0.1%	0.34	0.04%	ns	0.53	0.1%	<0.05
Liver	22.1	0.6%	20.9	1.5%	ns	19.6	0.6%	<0.05
Total	59.0	1.7%	52.1	3.0%	ns	80.3	6.6	<0.001

*All animals imaged 24 hr after ^{111}In injection.
†n = 4.
‡n = 3.
§Values in brackets expressed as ID/g.
¶Compared to uninjured.

NC) and the red blood cells were lysed. The PMN population was then analyzed using the fluorescence-activated cell sorter (FACS) and the mean fluorescence intensity for each sample was determined.

Statistical Analysis

A one-way analysis of variance with Newman-Keuls multiple range test was applied to compare the differences between multiple means.

RESULTS

Biodistribution of Indium-111-Labeled Immunoglobulins: Blood and Lungs

Table 1 shows that rats injected with ^{111}In*aICAM-1 showed a significant increase in the %ID/O in lungs both at 4 and 24 hr postbleomycin as compared to either uninjured animals (Table 1A) or rats that received ^{111}In*nmIgG (Table 1B) at the same times. In contrast, lung activity was not changed significantly at either 4 or 24 hr for ^{111}In*nmIgG rats (Table 1B). Injury progression caused a similar pattern for blood activity with both antibodies. The %ID/O for blood was reduced modestly at 4 hr and then almost doubled (~1.8-fold) at 24 hr postinjury.

The target-to-blood (T/B) ratio (computed from the %ID/g values in Table 1) was very high, 8/1 at 4 hr postinjury and 6/1 at 24 hr for ^{111}In*aICAM-1. These high T/B ratios suggest that injured lungs would be visible on scintigraphic images. In contrast for ^{111}In*nmIgG animals, the T/B ratios at 4 and 24 hr were less than 1, 0.5/1 and 0.4/1, respectively, which implies that injured lungs would not be scintigraphically visible.

Other Tissues

The spleen was the only other tissue besides the lung that was elevated as a function of bleomycin injury with ^{111}In*aICAM-1 (Table 1). Spleen uptake with the ^{111}In*nmIgG rats was not significantly elevated compared to the uninjured controls. In both ^{111}In*aICAM-1 and ^{111}In*nmIgG rats, heart activity was increased but only at 24 hr postinjury. Liver uptake for both antibodies was altered at 24 hr. The ^{111}In*aICAM-1 uptake dramatically increased (~1.8-fold), while ^{111}In*nmIgG localization declined modestly (12%) as injury progressed. The differences in the kidney uptake between the antibodies as a function of injury probably reflect the differences in the catabolic pathways for the two antibodies.

The %ID/g values for both antibodies (data not shown) followed these patterns except that the increase in splenic uptake for ^{111}In*nmIgG was significant at 24 hr. This meant that the %ID/g for heart and spleen was significantly increased at 24 hr for both antibodies (Table 1). To delineate the specificity of tissue localization for the two antibodies, a ratio, ^{111}In*aICAM-1/^{111}In*nmIgG × 100, was computed from the %ID/g data. This ratio increased significantly ($p < 0.001$) for spleen from 233 ± 23 in uninjured rats to 400 ± 38 at 24 hr. In contrast for heart, this value increased from 55 ± 13–69 ± 6 but not significantly($p > 0.15$). This demonstrates that at 24 hr, ^{111}In*aICAM-1 was elevated only for spleen excess of what was observed for the control immunoglobulin.

Table 1 demonstrates that a majority of activity for ^{111}In*aICAM-1 was deposited in the major organs for both uninjured and injured animals. The liver, kidney and spleen

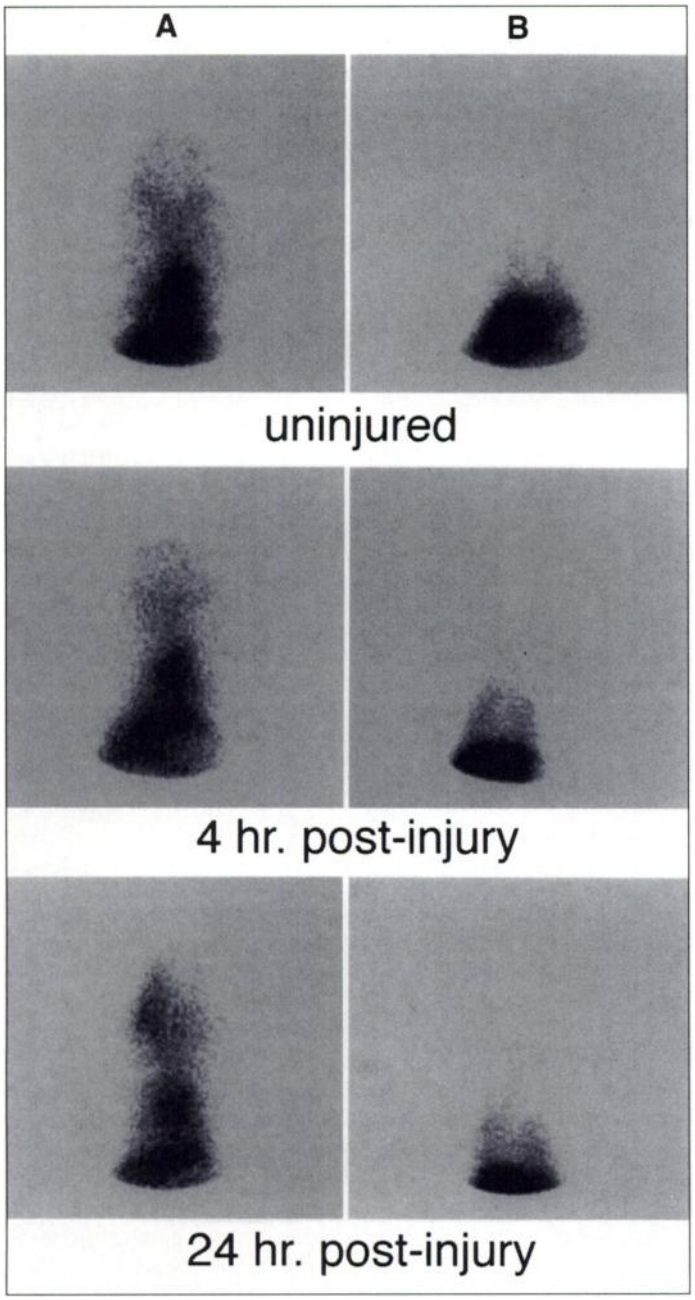

FIGURE 2. Pinhole scintigrams of the upper anterior torso of uninjured control rats and rats 4 and 24 hr postbleomycin injury injected with (A) ^{111}In*nmIgG or (B) ^{111}In*aICAM-1. The animals were imaged at 24 hr postinjection.

constituted ~50% of the ID and at 24 hr increased to ~84% mainly due an increase in liver activity. In contrast, for the ^{111}In*nmIgG rats, ~25% was present in these organs. The blood and liver contained the majority, > 47%, of the ID and also increased only at 24 hr to ~74%. This was due mainly to the elevation in blood ^{111}In.

Imaging of Indium-111-Labeled Immunoglobulins and Gallium-67-Citrate

The T/B data suggested that the lungs of rats injected with ^{111}In*aICAM-1, but not ^{111}In*nmIgG, could be visualized as early as 4 hr postbleomycin. Figure 2A shows that at 4 and 24 hr postinjury, rats injected with ^{111}In*nmIgG had only a high concentration of activity in the cardiac blood pool and liver. No activity appeared in the lung fields above tissue background. Images of the uninjured control animals were similar (Fig. 2). As the disease progressed (24 hr), the only change was the increase in activity in the area above the heart. This may relate to the blood activity increase or to the neck incision for the bleomycin injection. The images from the ^{67}Ga-citrate rats also showed no differences between injured and uninjured (data not shown). ROI analysis for the ^{111}In*nmIgG rats demonstrated no significant differences among the mean CPM/pixel/μCi values from uninjured and injured rats for all tissues (Table 2A).

In dramatic contrast, activity above background was clearly, uniformly visible in both lung fields in the ^{111}In*aICAM-1 rat imaged at 4 and 24 hr postbleomycin injury (Fig. 2B). Also, there was intense activity present in the liver. In the uninjured animals, only a very small amount of activity in the lungs above background was visible. There was also intense liver activity that is similar to the images of the injured rats. The images of the lungs at 4 and 24 hr can easily be distinguished from the uninjured. The values obtained from the ROI analysis support these observations (Table 2B). Both 4- and 24-hr values were elevated for injured lungs with a tendency toward significance and significantly, respectively. The liver values were 3-fold greater than the comparable values from the ^{111}In*nmIgG animals.

Expression of ICAM-1 on Lung Tissue

ICAM-1 up-regulation was demonstrated at 4 (Fig. 3C) and 24 (Fig. 3D) hr postinjury with increased fluorescence intensity apparent in the injured lung as compared to lung tissue from uninjured rats (Fig. 3B).

Expression of LFA-1α on Blood PMNs

The increase in LFA-1α expression on the PMNs from the bleomycin-treated animals at 4 (19%) and 24 (210%) hr was significantly increased compared to uninjured animals (Table 3).

DISCUSSION

Our results show that lung injury could be detected by ^{111}In*aICAM-1 as early as 4 hr postbleomycin by scintigraphic and biodistribution data. Lung injury could not be scintigraphically detected by ^{111}In*nmIgG at this time point or later. This 4-hr time point is critical in disease progression because it is very early in the injury stage. Lung histology, lung compliance and PMN influx into bronchoalveolar lavage fluid (BAL) are all within normal limits (*22,23*). Capillary permeability as measured by ^{111}In*nmIgG uptake (*24*) does not increase in the lung until 24 hr postinjury (Table 1B). It might be expected that aICAM-1 could interfere with PMN accretion. However, the concentration of this antibody in these experiments is very low, 10 μg, and should have no influence on the migration of WBCs into the inflamed area (*25*). These results suggest that ^{111}In*aICAM-1 has great potential to be a useful tool in the early detection of lung injury.

In addition, our data imply that the localization of ^{111}In*aICAM-1 is a specific event. Immunofluorescence data showed that ICAM-1 was up-regulated in the lung as a function of bleomycin injury. This up-regulation correlates well with both the biodistribution (Table 1A) and imaging data (Fig. 2). In addition, the enhanced expression of LFA-1α, the ICAM-1 counterreceptor, on blood PMNs postinjury is consistent with ICAM-1 up-regulation. The ability of the ^{111}In*aICAM-1 to be incorporated in the lung particularly at 4 hr postinjury also implies a specific process. In these biodistribution experiments, after the ^{111}In*aICAM-1 is injected, it is rapidly cleared from the blood (*17*). Because the animal was injured 4 hr before the 24-hr kill (Fig. 1), there is little of the antibody circulating at this time (Table 1A). Uptake by lung tissue is still high. Even

TABLE 2
Effect of Bleomycin-Induced Lung Injury on ROI Analysis of ^{111}In*nmIgG and ^{111}In*aICAM-1 Injected Rats

A. ^{111}In*aICAM-1	Time postbleomycin*							
	Uninjured†		4 hr‡			24 hr‡		
Tissue	ROI§	s.d.	ROI	s.d.	p value¶	ROI	s.d.	p value¶
Left lung	4.01	0.3	4.97	0.4		5.92	1.1	
Right lung	3.68	0.2	4.21	0.5		5.29	0.5	
Avg lung	3.84	0.3	4.59	0.4	$0.05 < p < 0.1$	5.61	0.7	<0.005
Liver	22.62	0.9	23.80	3.7	ns	27.36	7.2	ns
B. ^{111}In*nmIgG								
Left lung	1.45	0.1	1.31	0.2		1.46	0.3	
Right lung	1.37	0.1	1.68	0.2		1.53	0.4	
Avg. lung	1.41	0.1	1.49	0.2	ns	1.50	0.3	ns
Liver	8.95	0.03	8.95	0.9	ns	9.05	0.4	ns
Cardiac	8.42	0.1	7.77	0.9	ns	8.29	0.2	ns

*All animals imaged 24 hr post ^{111}In injection.
†n = 3.
‡n = 6.
§$\times 10^{-2}$CPM/pixel/μCi.
¶Compared to uninjured.

though the blood values for ^{111}In*nmIgG are >3-fold higher, giving rise to a greater diffusion driving force, the lung accretion was, however, much slower, requiring 24 hr. This suggests that ^{111}In*aICAM-1 is taken up in an active accretion process with a high density of antigen, namely ICAM-1.

A comparison of ^{111}In*aICAM-1 and ^{111}In*nmIgG uptake in spleen and liver, in addition to the lung, suggests that these increases were specific and not largely due to endothelial leakiness. Uptake by the spleen for ^{111}In*aICAM-1 preceded increased localization by ^{111}In*nmIgG (Table 1). While there was a small significant increase in spleen %ID/g for rats injected with ^{111}In*nmIgG at 24 hr postinjury, the ratio data showed that ^{111}In*aICAM-1 uptake was much greater. Thus, disruption of the endothelial barrier probably plays only a small role in the ^{111}In*aICAM-1 increase at 24 hr postinjury. There was a significant increase in ^{111}In*aICAM-1 localization for the liver only at 24 hr postinjury (Table 1). The increase in liver activity may also represent later disease changes in this model. Alternatively, because the liver is a repository of catabolized ^{111}In, this 24-hr difference may represent metabolic differences between the two antibodies. These data suggest that as a function of injury, ICAM-1 may be up-regulated early in the spleen and somewhat later in the liver.

In most antibody studies, as the antibodies are cleared from the blood, the T/B ratio usually improves (*19*). In this study with ^{111}In*aICAM-1, the T/B ratio did not improve as injury progressed and declined slightly (Table 1A). This decrease is not due to loss of activity from the injured lung, but because activity in the blood increased as a function of injury. This could be due to enhanced processing of the ^{111}In*aICAM-1 in the inflamed state and ^{111}In release. However, the blood activity increase appeared to be more dependent on this particular model because both antibodies yield an almost identical, ~1.7-fold, increase in activity (%ID/g data, Table 1). The bleomycin may damage the endothelial tissue allowing the extravascular

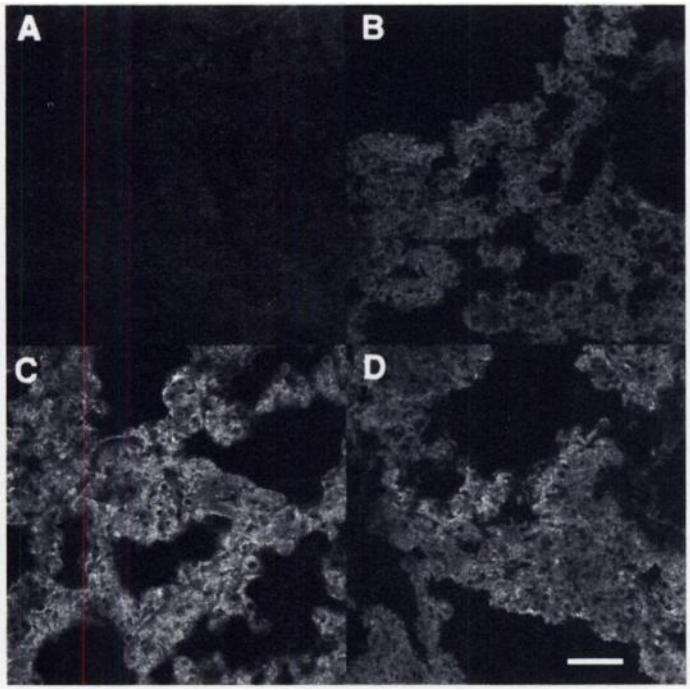

FIGURE 3. Expression of aICAM-1 immunofluorescence in cryostat sections of rat lung injured with bleomycin and uninjured rat lung. Sections were processed for immunofluorescence using: (A) no aICAM-1 first antibody as a control, (B) aICAM-1 as the first antibody in lung from uninjured rat, (C) lung from rats injured at 4 hr and (D) 24 hr before kill. A rhodamine-conjugated goat antimouse IgG was used as the second antibody in all sections. Magnification was 788-fold.

TABLE 3
Expression of LFA-1α on Rat Blood PMN After Bleomycin-Induced Lung Injury

	Anti-LFA-1α		
Sample	Mean fluorescent intensity*	s.d.	p value†
Uninjured	120	5.5	
4 hr postbleomycin	143	6.2	0.05
24 hr postbleomycin	372	7.4	0.001

*n = 2.
†Compared to uninjured.

^{111}In to return to the circulation. Alternatively, the plasma or blood volume might be reduced by the treatment. The cause of this increase is under active investigation in our laboratory.

This ^{111}In*aICAM-1 antibody has the potential to be used in patients in a similar manner as it was used in our model. In patients with high clinical suspicion, this antibody could be injected and images obtained until the lungs showed an indication of acute respiratory distress syndrome (ARDS) progression or the patient recovered. The acute stage of bleomycin-induced lung injury in rats mimics many of the conditions of acute lung injury in various patients including those with the ARDS. Early diagnosis is critical in any disease process and especially in ARDS because it is associated with a high death rate of 36%–65% (*26–28*). At present, once patients progress into ARDS there is no effective therapy only supportive management. The syndrome typically arises after a latency period of 72–96 hr after the inciting incident. This time period provides an opportunity to predict which high risk patients may develop ARDS and it also provides a time frame to begin potential therapy. Therapies may have failed in the past because of late initiation.

CONCLUSION

We have demonstrated that ^{111}In*aICAM-1 can detect the early stages of acute bleomycin-induced lung injury. Because ICAM-1 up-regulation is an early event in a variety of inflammatory processes and infections, we anticipate this antibody may have wide applications. While our data are very encouraging, it is necessary to demonstrate that similar results can be obtained in other models of inflammatory processes.

ACKNOWLEDGMENTS

This work was supported in part by Faculty Research Grants from the University of Connecticut Health Center. Preliminary accounts of this data have been presented previously (*29,30*).

REFERENCES

1. Alazraki NP. Gallium-67 imaging in infection. In: Early PJ, Sodee DB, eds. *Principles and practice of nuclear medicine*, 2nd ed. St Louis: Mosby; 1995:702–713.
2. Coleman RE, Datz FL. Detection of inflammatory disease using radiolabeled cells. In: Sandler MP, Coleman RE, Wackers F, et al., eds. *Diagnostic nuclear medicine*, 3rd ed. Baltimore: Williams and Wilkins; 1996:1509–1524.
3. Fischman AJ, Babich JW, Rubin RH. Infection imaging with Tc-99m-labeled chemotactic peptide analogs. *Semin Nucl Med* 1994;24:154–168.
4. van der Laken CJ, Boerman OC, Oyen WJG, et al. Specific localization of radioiodinated human recombinant interleukin-1 in infectious foci [Abstract]. *J Nucl Med* 1995;36:229P–230P.
5. Moyer BR, Vallabhjosula S, Lister-James J, et al. Technetium-99m-white blood cell specific imaging agent developed from platelet factor 4 to detect infection. *J Nucl Med* 1996;37:673–679.
6. Goodbody A, Ballinger J, Tran L, et al. A new technetium-99m-labeled peptide inflammation imaging agent. *Eur J Nucl Med* 1994;21:790.
7. Becker W, Blair J, Behr T, et al. Detection of soft-tissue infections and osteomyelitis using technetium-99m-labeled anti-granulocyte monoclonal antibody fragment. *J Nucl Med* 1994;35:1436–1443.
8. Zimmerman GA, Prescott SM, McIntyre TM. Endothelial cell interactions with granulocytes: tethering and signaling molecules. *Immunol Today* 1992;13:93–100.
9. Argenbright LW, Barton RW. Interactions of leukocyte integrins with intercellular adhesion molecule 1 in the production of inflammatory vascular injury in vivo. *J Clin Invest* 1992;89:259–272.
10. Gearing AJH, Newman W. Circulating adhesion molecules in disease. *Immunol Today* 1993;14:506–512.
11. Smith CW, Marlin SD, Rothlein R, et al. Cooperative interactions of LFA-1 and Mac-1 with intercellular adhesion molecule-1 in facilitating adherence and transendothelial migration of human neutrophils in vitro. *J Clin Invest* 1989;83:2008–2017.
12. Pohlman TH, Stanness KA, Beatty PG, et al. An endothelial cell-surface factor induced in vitro by lipopolysaccharide, interleukin-1 and tumor necrosis factor increases neutrophil adherence by a CDw18-dependent mechanism. *J Immunol* 1986;136:4548–4553.
13. Wellicome SM, Thornhill MH, Pitzalis C, et al. A monoclonal antibody that detects a novel antigen on endothelial cells and is induced by TFNα, IL-1 or LPS. *J Immunol* 1990;144:2558–2565.
14. Luscinskas FW, Cybulsky MI, Keily J-M, et al. Cytokine-activated human endothelial monolayers support enhanced neutrophil transmigration via a mechanism involving both endothelial-leukocyte adhesion molecule-1 and intercellular adhesion molecule-1. *J Immunol* 1991;146:1617–1625.
15. Norris P, Poston RN, Thomas S, Thornhill M, Hawk J, Haskard DO. The expression of endothelial leukocyte adhesion molecule-1 (ELAM-1), intercellular adhesion molecule-1 (ICAM-1) and vascular cell adhesion molecule-1 (VCAM-1) in experimental cutaneous inflammation: a comparison of ultraviolet B erythema and delayed hypersensitivity. *J Invest Dermatol* 1991;96:763–770.
16. Leeuwenberg JFM, Smeets EF, Neefjes JJ, et al. E-selectin and intercellular adhesion molecule-1 are released by activated human endothelial cells *in vitro*. *Immunology* 1992;77:543–549.
17. Sasso D, Gionfriddo M, Thrall R, Syrbu S, Smilowitz H, Weiner R. Biodistribution of ^{111}In-labeled antibody directed against intracellular adhesion molecule-1 in normal rats. *J Nucl Med* 1996;37:656–661.
18. Fischman AJ, Rubin RH. Radiolabeled nonspecific human polyclonal immunoglobulin G for imaging focal inflammation. In: Sandler MP, Coleman RE, Wackers F, et al., eds. *Diagnostic nuclear medicine*, 3rd ed. Baltimore: Williams and Wilkins; 1996: 1525–1533.
19. Serafini AN. Clinical applications of monoclonal antibody imaging. In: Sandler MP, Coleman RE, Wackers F, et al., eds. *Diagnostic nuclear medicine*, 3rd ed. Baltimore: Williams and Wilkins; 1996:1275–1291.
20. Thrall RS, McCormick JR, Jack RM, McReynolds RA, Ward PA. Bleomycin-induced pulmonary fibrosis in the rat. *Am J Pathol* 1979;95:117–127.
21. Ussov WY, Peters AM, Hodgson HJF, Hughes JMB. Quantification of pulmonary uptake of indium-111-labeled granulocyte in inflammatory bowel disease. *Eur J Nucl Med* 1994;21:6–11.
22. Grunze MF, Parkinson D, Sulavik SB, Thrall RS. The effect of steroid treatment on changes in volume pressure curves after bleomycin-induced lung injury in the rat. *Exp Lung Res* 1988;14:183–195.
23. Thrall RS, Barton RW, D'Amato DA, Sulavik SB. Differential cellular analysis of bronchoalveolar lavage fluid obtained at various stages during the development of bleomycin-induced pulmonary fibrosis in the rat. *Am Rev Respir Dis* 1982;126:488–492.
24. Oyen WJG, Boerman OC, van der Laken CJ, Classens RAMJ, van der Meer JWM, Corstens FHM. The uptake mechanisms of inflammation-and infection-localizing agents. *Eur J Nucl Med* 1996;23:459–465.
25. Smith RJ, Chosay JG, Dunn CJ, Manning AM, Justen JM. ICAM-1 mediates leukocyte-endothelium adhesive interactions in the reversed passive Arthus reaction. *J Leukoc Biol* 1996;59:333–340.
26. Milberg JA, Davis DR, Steinberg KP, Hudson LD. Improved survival of patients with acute respiratory distress syndrome (ARDS): 1983–1993. *JAMA* 1995:273:306–309.
27. Murray JF, Matthay MA, Luce JM, Flick MR. An expanded definition of adult respiratory distress syndrome. *Am Rev Respir Dis* 1988;138:720–723.
28. Villar J, Slutsky AS. The incidence of the adult respiratory distress syndrome. *Am Rev Respir Dis* 1989;140:814–816.
29. Sasso D, Gionfriddo M, Syrbu S, Smilowitz H, Thrall R, Weiner R. Early detection of ARDS using indium-111-labeled anti-intercellular adhesion molecule-1 in a rat model. *J Nucl Med* 1995;36:159P.
30. Sasso D, Thrall R, Vento J, Weiner R. Early detection of lung injury in rat models using indium-111-labeled anti-intercellular adhesion molecule-1 [Abstract]. *J Nucl Med* 1996;37(suppl):196P.